

Nonlocal vs. Diffusion Mechanisms of Electron Cyclotron Radiation Transport in Fusion Reactor-Grade Tokamaks

K.V. Cherepanov,¹ A.B. Kukushkin,¹ P.V. Minashin,^{1,2} V.S. Neverov^{1,2}

¹*NFI RRC "Kurchatov Institute", Moscow, 123182, Russia*

²*Moscow Engineering Physics Institute, Russia*

1. Introduction. The necessity to model the operation of reactor-grade tokamaks ($\langle T_e \rangle > 10\text{keV}$, $B_T > 5\text{T}$, reflectivity of electron cyclotron radiation (ECR) from the walls $R_W > 0.5$) with fast-routine transport codes requires parameterization of the distribution, over magnetic surfaces, of ECR local net power loss, $P_{EC}(\rho)$. The requested accuracy of parametric representations is determined by the recent recognition of the significance of ECR contribution to local energy balance in the central part of the plasma column in the steady-state scenarios of tokamak ITER operation, that was shown [1] via coupling the ECR transport fast-routine code CYTRAN [2(A)] with tokamak global transport code ASTRA. On the basis of calculations with the code CYNEQ [3], a simple semi-analytic description of $P_{EC}(\rho)$ was proposed [4], which modifies and simplifies the fast routine code CYTRAN and may be used in transport calculations for tokamak-reactors ITER and DEMO.

Here we analyze the accuracy of the approach [4] with respect to (i) analytic calculation of the boundary of “optically thick” core, including the effects of spectral non-monotonic dependence of this boundary, (ii) spatial averaging of absorption/emission characteristics in the nonlocality-based approaches [2,3], and (iii) relative contribution of nonlocal (non-diffusion) and diffusion mechanisms of ECR transport.

2. Spectral dependence of the boundary of “optically thick” core. The ECR transport in reactor-grade tokamaks with highly reflecting walls and non-circular cross section of toroidal plasma column was reduced to a 1-D transport problem [2(A)], in which the boundary of “optically thick” core, $\rho_{cut}(\omega)$, in the EC radiation’s reduced phase space {frequency ω , effective minor radius $\rho \in [0,1]$ }, is defined by equation

$$\tau_{crit} = \int_{\rho_{cut}(\omega, K)}^1 \chi_K(\rho, \omega) d\rho, \quad (1)$$

where χ_K is the normalized absorption coefficient, averaged over radiation angles, for extraordinary (K=X) and ordinary (K=O) waves, and the optical thickness of outer *transparent* layer, $\tau_{crit} = 1.5$, was suggested in [2(A)] to fit the results of Monte-Carlo simulations [2(B)]. In CYNEQ, instead of using the fitting formulas [2(A)] for $\chi_K(\omega, T_e(\rho))$

in maxwellian plasma, the curves $\rho_{\text{cut}}(\omega, K)$ are calculated straightforwardly (and for arbitrary electron velocity distribution). This gives non-monotonic behavior (Fig. 1), caused by only partial overlapping of Doppler-broadened spectral lines at low- and moderate-number harmonics of ECR. For maxwellian plasmas, $\rho_{\text{cut}}(\omega, K)$ may be approximated linearly - Eqs. (5),(6) in [4]. The latter was suggested by our calculations with the fitting formulas [2(A)] for χ_K (accurate to $\sim 20\%$ for $10 < T_e < 120$ keV [2(A)]), which were modified in [4] to avoid their loss of accuracy at $T_e < 10$ keV.

A comparison of $\rho_{\text{cut}}(\omega, K)$ (Fig. 1) and respective comparison of spectral intensities and power loss profiles $P_{\text{EC}}(\rho)$ (Fig. 2) are given for electron density and temperature profiles

$$n_e(\rho) = n_e(1) + (n_e(0) - n_e(1)) [1 - \rho^{\beta_n}]^{\gamma_n}, T_e(\rho) = T_e(1) + (T_e(0) - T_e(1)) [1 - \rho^{\beta_T}]^{\gamma_T}, \quad (2)$$

taken close to ITER scenarios -- “inductive” in [5] and “steady-state-2” in [1]. Their parameters are given below, where major/minor radii, density, temperature and toroidal magnetic field are in m, 10^{20} m^{-3} , keV, and Tesla, respectively.

Regime	R	a	$B_T(0)$	$n_e(0)$	$n_e(1)$	$T_e(0)$	$T_e(1)$	γ_n	β_n	γ_T	β_T	R_w
Inductive	6.2	2	5.3	1	0.5	25	2	0.1	2	1.5	2	0.6
SS-2 [1]	6.4	1.9	5.2	0.7	0.175	46	3	0.1	2	4	4	0.6

The profile of *total* magnetic field, averaged over magnetic surfaces, is taken flat: $B_{\text{tot}}(\rho) = B_T(0)$, that, e.g., for inductive regime is accurate to $< 20\%$ [5].

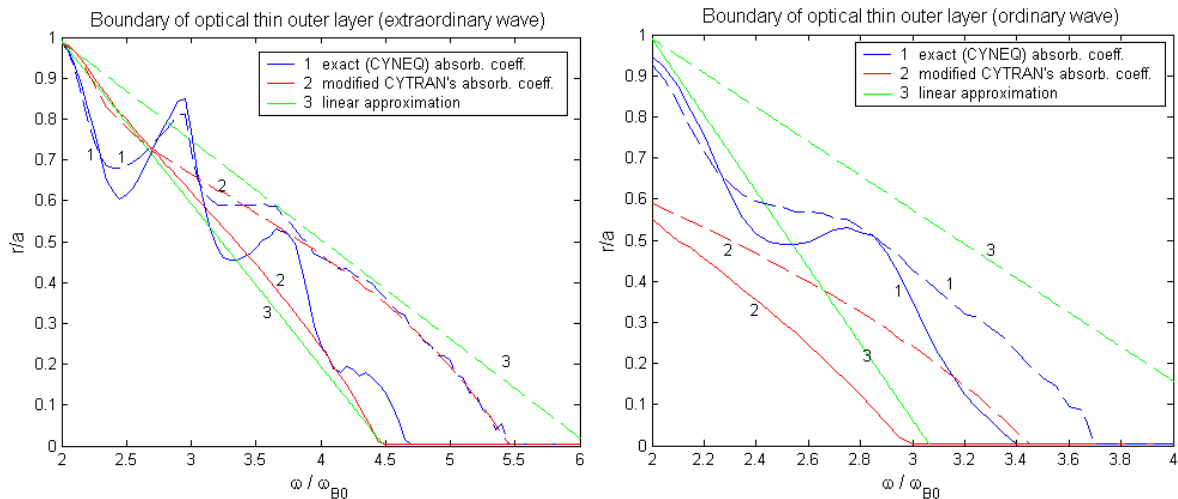


Fig. 1. Comparison of $\rho_{\text{cut}}(\omega)$ for extraordinary (left) and ordinary (right) EC waves for “inductive” regime (solid) and “steady-state-2” regime (dashed). The EC frequency ω_{B0} is defined for $B = B_T(0)$. Curves 1 - calculation with exact χ_K (CYNEQ); 2 - calculation with fitting formula for χ_K [2(A)], modified in [4]; 3 - linear approximation [4].

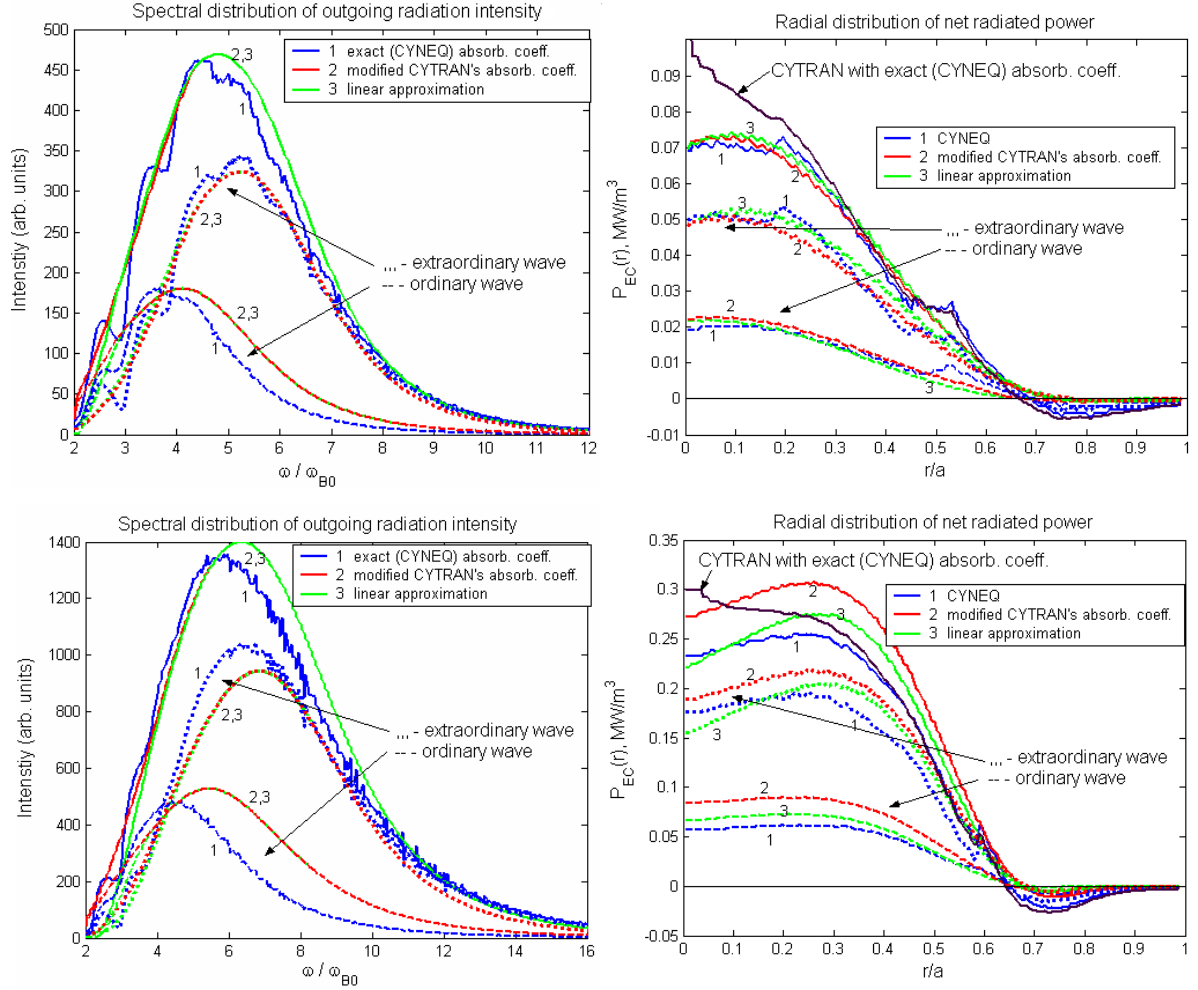
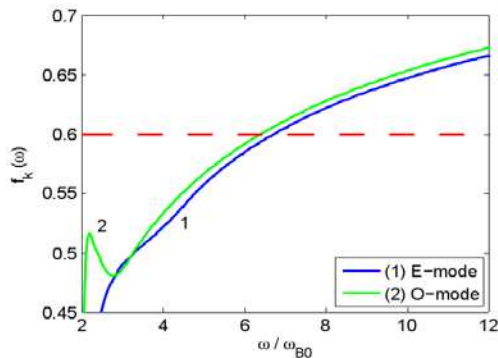


Fig. 2. Comparison of spectral intensities of outgoing radiation (left) and power loss profiles $P_{EC}(\rho)$ (right) for “inductive” regime (upper) and “steady-state-2” regime (lower).

3. Spatial averaging of absorption characteristics. Analytic approximation for spectral temperature of EC radiation, $T_{ECR}(\omega, K)$ in Eq.(1) in [4], was resulted from the following substitution in CYNEQ’s formalism (cf. Eq.(4) in [4] and denominator in Eq.(2) in [6])

$$2 \int_{\rho_{cut}}^1 \chi_K(\omega, T_e(\rho)) \rho d\rho = \chi_K(\omega, f T_e(\rho_{cut}(\omega, K)) + (1 - f) T_e(1)) (1 - \rho_{cut}^2), \quad (3)$$

which assumes neglect of spectral and mode dependence of factor f . $f(\omega, K)$ as a solution of



Eq.(3) for “inductive” regime is shown in Fig.3.

Sensitivity of $T_{ECR}(\omega, K)$ and $P_{EC}(\rho)$ to a variation of factor f , taken a constant, is shown in Fig. 4.

Fig. 3. Spectral dependence of factor f , defined by Eq.(3) and responsible for spatial averaging of electron temperature in $T_{ECR}(\omega, K)$, for “inductive” regime. Value $f(\omega, K) = \text{const} = 0.6$ is the choice of analytic description of $P_{EC}(\rho)$ in [4].

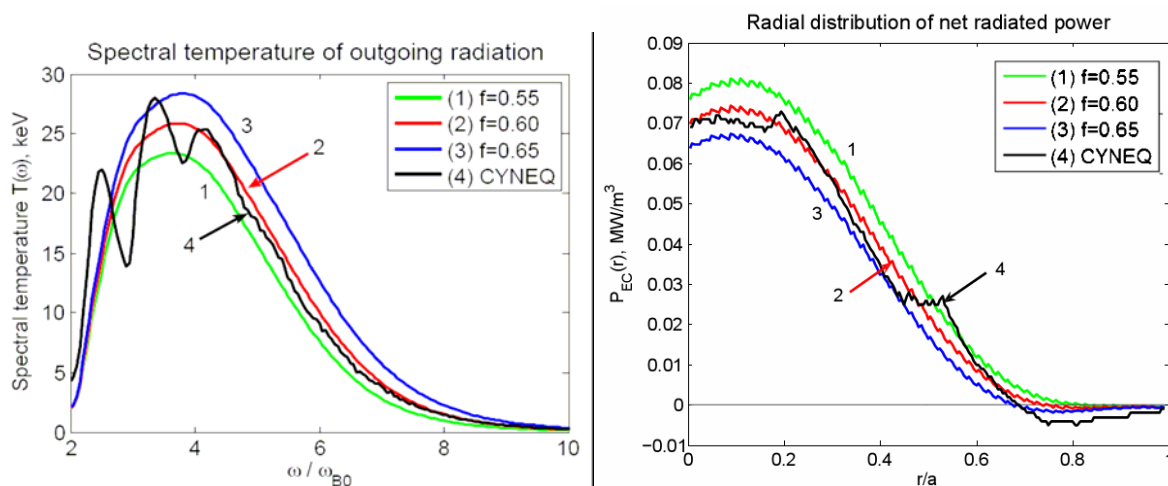


Fig. 4. Dependencies of total spectral temperature of outgoing radiation, $T_{ECR}(\omega, E+O)$, (left) and of power loss profiles $P_{EC}(\rho)$ (right) on the factor f , taken a constant.

4. Relative contribution of nonlocal (non-diffusion) and diffusion mechanisms to $P_{EC}(\rho)$. Besides above characteristics of non-locality of ECR transport (Secs. 2,3), there is the most direct evidence for nonlocality, which shows the effect of the neglect of the contribution [2(A)] of diffusive transport of ECR in “optically thick” core (which is located lower the curves in Fig. 1) to power loss profiles $P_{EC}(\rho)$. Such a neglect in CYNEQ (cf. Eq.(2) in [6]) underestimates $P_{EC}(\rho)$ in the central part of plasma column, as compared to CYNEQ’s calculations with restored contribution [2(A)] of ECR diffusion in the core (see black curves in Fig.2, right column). The difference lies within the accuracy of the approach [2(A)].

5. Conclusion. Analysis of accuracy of the approach [4] with respect to its nonlocal characteristics illustrates dominance of nonlocality of ECR transport, in particular, in spatial profile of EC net radiated power for typical conditions of magnetic fusion reactor.

Acknowledgments. The work is partly supported by the Russian Federal Program of Support of Leading Scientific Schools’ Researches (grant NSH-9878.2006.2).

REFERENCES

- [1] Albajar F., Bornatici M., Cortes G., *et al.*, Nucl. Fusion, 45 (2005) 642.
- [2] Tamor S., (A) Repts. SAI-023-81-110-LJ/ LAPS-72 and SAI-023-81-189-LJ/ LAPS-72, La Jolla, CA: Science Applications (1981); (B) Fusion Technol., 3 (1983) 293; Nucl. Instr. and Meth. Phys. Res., A271 (1988) 37.
- [3] Cherepanov K.V., Kukushkin A.B., Proc. 31st EPS Conf. Plasma Phys. Contr. Fusion. (London, U.K., 2004), ECA vol. 28G, P-1.175; Proc. 20th IAEA Fusion Energy Conf. (Vilamoura, 2004), TH/P6-56.
- [4] Cherepanov K.V., Kukushkin A.B., Proc. 33rd EPS Conf. Plasma Phys. Contr. Fusion. (Rome, Italy, 2006), P-1.169.
- [5] Polevoi A.R., Medvedev S.Yu., Mukhovatov S.V., *et. al.*, J Plasma Fusion Res. SERIES, 5 (2002) 82-87.
- [6] Kukushkin A.B., Proc. 24th EPS Conf. Contr. Fusion Plasma Phys., Berchtesgaden, 1997, ECA vol. 21A, Part II, 849.